Abnormal meibum is associated with *SREBF1* mutation and IFAP syndrome 2

Igor A. Butovich[a,*], Martha Schatz[b], Ujwala S. Saboo[b], Jadwiga C. Wojtowicz[a,*], Daniel A. Johnson[b]

[a] University of Texas Southwestern Medical Center, Dallas, TX, USA
[b] University of Texas Health Science Center in San Antonio, San Antonio, TX, USA

***Address for correspondence:** Igor A. Butovich, PhD, Department of Ophthalmology, UTSouthwestern Medical Center, 5323 Harry Hines Blvd., Dallas, TX, 75390-9057, USA
Phone: +1 (214) 648-3523; E-mail: igor.butovich@utsouthwestern.edu

Abstract

The X-linked Ichthyosis Follicularis, Alopecia, and Photophobia syndrome type 2 (IFAP2), is a condition that has been linked to an Arg527-to-Cys mutation in the *SREBF1* gene. However, the molecular implications of the mutation in Meibomian glands remained unknown. Our goals were to elucidate the biochemical factors associated with the disease, and allow for unbiased diagnoses of the condition. Normal human meibum samples and abnormal specimens from a patient with IFAP2-like signs and symptoms were collected from Meibomian glands of the donors. Genetic analysis of the abnormal subject uncovered the mutation that was reported for IFAP2. The meibum samples were analyzed qualitatively and quantitatively using liquid chromatography/mass spectrometry (LC/MS), and, then, compared using various multivariate statistical approaches. LC/MS analyses provided detailed information on the differences in lipidomic profiles of normal and abnormal meibum samples, specifically saturated and unsaturated wax esters (SWE and UWE). Abnormal meibum has been shown to be highly enriched with SWE, which increased the SWE/UWE ratio to highly abnormal levels. The higher melting temperature of SWE compared with that of UWE correlated well with the clinical observations of poor expressibility and abnormal appearance of abnormal meibum. Our study demonstrated that upregulation of SWE in abnormal meibum may be associated with severe Meibomian gland dysfunction caused by the *SREBF1* mutation. LC/MS can be used as a sensitive and informative tool that can uncover minute differences in the Meibomian lipidomes of subjects with Meibomian gland dysfunction and the results can be used to pinpoint their molecular causes and markers.

* Visiting Assistant Professor from Centro Oftalmologico de Valencia, Avenue Bolivar Norte, Edificio Torre Venezuela, Valencia, Carabobo, Venezuela.

Keywords

Lipid metabolism; Meibomian glands; meibum; Meibomian gland dysfunction; ophthalmology, gene mutations; SREBF1; IFAP syndrome 2; wax esters; metabolic disorders

Introduction

Various ocular surface diseases (OSD), such as Meibomian gland dysfunction (MGD) and dry eye (DE), have a strong detrimental impact on vision and quality of life of affected individuals (Lin et al., 2024; Valdes-Arias et al., 2024), and represent a considerable financial burden (Mizuno et al., 2012; Yu et al., 2011). Therefore, OSD are important targets for developing new treatments. However, the multifactorial nature of MGD and DE requires targeted approaches not only for their treatment, but also for their reliable and objective diagnosis, which, currently, relies on clinical observations and testing more than on biochemical or genetic/genomic approaches. The insufficient knowledge of the molecular mechanisms of the onset of the diseases usually precludes medical practitioners and biomedical scientists from developing personalized treatments for the patients. In many cases, OSD in general, and MGD/DE specifically, are associated with either insufficient production of meibum or its abnormal composition (Narang et al., 2023; Stapleton et al., 2025). The role of the latter is a subject of this paper.

Methods

Meibum collection procedures were approved by the Institutional Review Board of the UT Southwestern Medical Center in Dallas, TX (UTSW). The collection procedures were performed in accordance with the principles of the Declaration of Helsinki. Written informed consents were obtained. Standard ophthalmic approaches, such as answering OSDI questionnaire, slit lamp evaluation of the ocular surface, MG, and adnexa, Schirmer's tests were used to determine if the subjects had signs and symptoms of MGD/DE. The samples from an abnormal female subject with severe MGD were collected at the University of Texas Health Science Center at San Antonio, TX (UTHSCSA) as de-identified medical procedure discards. Meibum was collected by expressing the secretion from eyelids of the subjects as described before (Butovich, 2008). Seven normal human meibum samples were collected at UTSW, while abnormal specimens were collected from a subject with severe MGD at UTHSCSA. Meibum was sampled from each of the four eyelids of the abnormal subject and analyzed separately without pooling.

The analyses of meibum were conducted using reverse phase liquid chromatography in combination with high-resolution atmospheric pressure chemical ionization (APCI) mass spectrometry (LC/MS) (Butovich et al., 2023). The lipid components of meibum were detected and identified on the basis of their mass-to-charge ratios (*m/z*), LC retention times, and MS/MS fragmentation patterns.

Where possible, the results were compared with those for commercially available authentic lipid standards.

The individual lipids analyzed in the study were normalized against the total lipid content in their respective meibum samples and presented in the paper either as relative ion abundances, or as fold changes between the study samples (Butovich et al., 2023). This approach compensated for uneven physical sizes of collected meibum specimens without the need to know their exact weights. The data were analyzed in three different ways conducting: 1) untargeted, unbiased, unsupervised Principal Component Analysis (PCA); 2) Orthogonal Projections to Latent Structures Discriminant Analysis (OPLS-DA) approach; and 3) targeted analyses of selected lipid species. The PCA and OPLS-DA analyses of the raw LC/MS data were performed using the Progenesis QI and EZinfo software packages, while targeted analyses were conducted as described before (Butovich and Wilkerson, 2022; Butovich et al., 2023) using the MassLynx and MS^E DataViewer (all from Waters Corp., Milford, MA, USA). The targeted analyses were conducted using SigmaPlot version 11 (from Systat Software Inc., Chicago, IL, USA), and the results were compared using Student's t-test (for two groups of samples) or one-way ANOVA (for multiple groups of samples).

Results and discussion

Clinical evaluation of normal human subjects revealed no symptoms or signs of DE/MGD and no reported systemic diseases that would affect their vision or general lipid metabolism. The abnormal subject was a 1-5-yr old female. The history of present illnesses included bilateral corneal opacity (**Figure 1A**), photophobia, debris in the tear film, and severe MGD. The subconjunctival Kenalog injections and oral Prednisolone Forte were ineffective in alleviating the conditions. At the same time, the patient had signs of cyclic alopecia in the scalp, eyebrows and eyelashes, which implied a systemic skin- and hair-growth related disorder(s), such as atopic dermatitis. The patient was negative for Herpes simplex, Cytomegalovirus, and syphilis. The lipid panel of the subject was within normal limits. The results of the corneal impression cytology and lid margin cultures were also within normal limits and negative for fungal and staphylococcus infections. However, the patient had cloudy, scarred, neovascularized corneas, and clearly abnormal white tubular MG secretions in both eyes (**Figures 1B**) characteristic of MGD.

Initial comparative analysis of abnormal vs. normal meibum showed little differences between the specimens: neither their total ion chromatograms, nor observation mass spectra were visibly

different (**Figures 1C-1F**). However, the unbiased, unsupervised, multivariate PCA demonstrated that the study samples formed two separate, non-overlapping clusters (**Figure 1G**), which implied substantial differences in their lipid compositions.

To explore what those differences might be, the data were re-analyzed using the more focused OPLS-DA approach, and a range of statistical tests were performed. First, the Variable Importance plot (VIP) was generated, which allowed us to identify 10 most influential lipids that had highest impact on the separation of the study groups (**Figure 1H**). The analysis of elemental composition of those lipids was performed using the EleComp software (from Waters) and suggested that they were mostly saturated and unsaturated wax esters (SWE and UWE, correspondingly). Their identities were verified using LC retention times and MS/MS fragmentation patterns. The following marker WE were identified: *m/z* 617.6192– $C_{42}H_{80}O_2$ (di-UWE); *m/z* 619.6389 – $C_{42}H_{82}O_2$ (mono-UWE); *m/z* 621.6212 – $C_{42}H_{84}O_2$ (SWE); *m/z* 633.6522 – $C_{43}H_{84}O_2$ (mono-UWE); *m/z* 635.6400 – $C_{43}H_{86}O_2$ (SWE); *m/z* 645.6551 – $C_{44}H_{84}O_2$ (di-UWE); *m/z* 647.6690 – $C_{44}H_{86}O_2$ (mono-UWE); *m/z* 649.6493 – $C_{44}H_{88}O_2$ (SWE); *m/z* 673.6838 – $C_{46}H_{90}O_2$ (mono-UWE); and *m/z* 675.6879 – $C_{46}H_{92}O_2$ (SWE). All compounds were detected as H^+ adducts using atmospheric pressure chemical ionization MS (APCI MS) (Butovich and Suzuki, 2020).

However, the VIP does not answer a question "*Which* lipids were overexpressed in *which* type of meibum?". To obtain this information, the most common approach is to use the S-Plot (**Figure 1I**). The lipids shown in the lower left quadrant of the graph, such as UWE, are highly expressed in the meibum of normal subjects, while those shown in the upper right quadrant – SWE – are markers of the abnormal meibum. These lipids were the most prominent discriminating factors between the study groups.

Still, the S-plot did not answer another important question "What are the *fold changes* of those lipids in different types of meibum?" To find the answer, we subjected the samples to a more focused approach, targeting a few representative WE from both study groups (**Figure 2**). The results of the analyses of two representative WE – a saturated compound $C_{42}H_{84}O_2$ and a monounsaturated $C_{42}H_{82}O_2$ – are shown in **Figures 2A1-2D2** as extracted ion chromatograms (EIC) and mass spectra. Clearly, the apparent ratios of the two WE were opposite in normal and abnormal meibum, and so were the ratios of other SWE and UWE (not shown).

A comprehensive evaluation of all differences between the two types of meibum goes beyond the scope of this paper and will be reported elsewhere. For this study, we characterized the lipid specimens concentrating on the gross differences between their fatty acids (FA) – essential components of cholesteryl esters (CE) and WE– using LC/MS with in-source fragmentation of lipid ions. The EIC of

two major FA – palmitic acid ($C_{16:0}$) and oleic acid ($C_{18:1}$) – revealed the dominance of $C_{16:0}$-based lipids in abnormal meibum, and $C_{18:1}$-based lipids in the normal one (**Figures 2E1 and 2E2**).

To quantitate the differences, the EIC of three major FA and nine major WE were plotted, integrated and summed up, and the apparent balances between the compounds were determined (**Figures 2F and 2G**). Both experiments revealed the same trend in abnormal meibum – a multifold increase in the fractions of saturated FA and WE and a decrease in unsaturated lipids. Thus, the results of the untargeted analyses of intact Meibomian lipids were supported by these more targeted approaches.

The final question was "What could the reasons for such dramatic changes in the Meibomian lipidome of the abnormal subject be?" The magnitude of molecular changes and clinical signs was large enough to suspect a genetic mutation in a gene that regulates lipid metabolism in MG. Therefore, the genomic testing was warranted and performed at UTHSCSA. During a full exome analysis, a CGC-to-TGC heterozygous C>T mutation in the *SREBF1* gene in exon 8 (R527C) was discovered that has been linked to a previously described abnormality called X-linked Ichthyosis Follicularis, Alopecia and Photophobia syndrome type 2 (or IFAP2) (Hamm et al., 1991; Wang et al., 2020).

The IFAP2 syndrome mutation in *SREBF1* gene have been linked to various abnormalities, including ocular and skin phenotype (Cursiefen et al., 1999). The mutation may affect S1P recognition and cleavage. Our initial clinical findings on the abnormal subject in 2018-2019 were in line with signs and symptoms of IFAP2 syndrome, while our current lipidomic data revealed the detrimental effect of the mutation on meibogenesis in MG (Butovich, 2017) – a dramatic increase in the SWE/UWE ratios. It is well known that SWE have considerably higher melting temperatures than their unsaturated counterparts of the same length (Patel et al., 2001). Thus, the multifold increase in the abundance of SWE is one of the likely reasons of the anomalous properties of meibum reported here, which may have negative downstream impact on the ocular surface health of the abnormal subjects.

Conclusions

Our experiments established that IFAP2 syndrome is associated with a dramatic imbalance in the profiles of saturated and unsaturated wax esters in meibum. Sophisticated bioanalytical techniques such as LC/MS can, and should, be incorporated in clinical practice on a wider scale as they can provide valuable information on the molecular mechanisms of pathologies and their markers, and complement clinical approaches, to ensure proper diagnosing and selection of treatments for patients.

Authorship contribution statement

I. A. Butovich: Conceptualization, experimentation, data acquisition and analysis, writing and reviewing the manuscript, supervision, project administration, funding acquisition (at UTSW).
M. Schatz: Clinical testing and sample collection, data analysis, reviewing the manuscript.
U. S. Saboo: Clinical testing and sample collection, data analysis, reviewing the manuscript.
J. C. Wojtowicz: Clinical testing and sample collection, data analysis, reviewing the manuscript.
D. A. Johnson: Conceptualization, data acquisition, supervision, project administration, and funding acquisition (at UTHSCSA).

Funding statement

This study was supported in part by an R01 grant EY027349 from the National Institutes of Health to Dr. I. A. Butovich, and by a Challenge Grant from the Research to Prevent Blindness (New York, NY) to the Department of Ophthalmology of UTSW. The funding organizations had no role in the design and conduct of the study.

Declaration of competing interests

The authors have no conflicts of interests to declare.

Data statement

All relevant data are included in the manuscript. Additional data can be requested from the corresponding author (I. A. Butovich).

Figure legends

Figure 1. The R527C mutation in *SREBF1* is associated with corneal opacification, inspissated meibum, and accumulation of abnormal lipids in Meibomian gland secretions.

(A) Abnormal cornea and *(B)* Meibomian gland secretions of the pediatric patient with a *SREBF1* mutation. The cloudy portion of the cornea and tubular Meibomian gland secretions are marked with

white and black arrows. *(C-I)* Unbiased, untargeted, unsupervised lipidomic analyses of normal and abnormal meibum using liquid chromatography–APCI mass spectrometry. *(C)* A total ion chromatogram of a representative normal human meibum sample. *(D)* An observation mass spectrum of the normal human meibum sample from panel A. *(E)* A total ion chromatogram of an abnormal human meibum sample. *(F)* An observation mass spectrum of the abnormal human meibum sample from Panel C. *(G)* A PCA plot demonstrated clear separation of the abnormal samples from the normal ones. *(H)* A Variable Importance Plot was generated using the OPLS-DA approach and identified ten most statistically influential lipids that were responsible for differentiation of normal and abnormal study samples. *(I)* A S-Plot was used to identify lipids that could be considered markers of normal and abnormal meibum. Lipids in the lower right quadrant were highly expressed in normal meibum, while lipids from the upper left quadrant were overexpressed in the abnormal secretions.

Figure 2. Targeted lipidomic analyses of saturated and unsaturated wax esters and fatty acids detected in normal and abnormal study samples.

(A1) LC/MS detection of a saturated wax ester (SWE) $C_{42}H_{84}O_2$ in normal meibum. The LC retention time and the peak area are shown next to the peak. *(A2)* The mass spectrum of the compound shown in Panel A1. *(B1)* Mono-unsaturated wax ester $C_{42}H_{82}O_2$ in normal meibum. *(B2)* The mass spectrum of the compound shown in Panel B1. *(C1)* Saturated wax ester (SWE) $C_{42}H_{84}O_2$ in abnormal meibum. *(C2)* The mass spectrum of the compound shown in Panel C1. *(D1)* Unsaturated wax ester (SWE) $C_{42}H_{82}O_2$ in abnormal meibum. *(D2)* The mass spectrum of the compound shown in Panel D1. *(E1)* Extracted ion chromatograms of $C_{16:0}$ palmitic acid fragments in Meibomian lipids of normal (black trace) and abnormal (red trace) meibum. The results were generate using in-source fragmentation of intact lipids in MS^E experiments. *(E2)* Extracted ion chromatograms of $C_{18:1}$ oleic acid fragments in Meibomian lipids of normal (black trace) and abnormal (red trace) meibum. The total lipid contents of the samples were the same. *(F)* Balance between palmitic (*m/z* 257) and oleic (*m/z* 283) FA residues in normal and abnormal meibum. *(G)* Balance between saturated, monounsaturated, and diunsaturated wax esters in normal and abnormal meibum.

References

Butovich, I.A., 2008. On the lipid composition of human meibum and tears: comparative analysis of nonpolar lipids. Invest Ophthalmol Vis Sci 49, 3779-3789. https://doi.org/10.1167/iovs.08-1889.

Butovich, I.A., 2017. Meibomian glands, meibum, and meibogenesis. Exp Eye Res 163, 2-16. https://doi.org/10.1016/j.exer.2017.06.020.

Butovich, I.A., Suzuki, T., 2020. Delineating a novel metabolic high triglycerides-low waxes syndrome that affects lipid homeostasis in meibomian and sebaceous glands. Exp Eye Res 199, 108189. https://doi.org/10.1016/j.exer.2020.108189.

Butovich, I.A., Wilkerson, A., 2022. Dynamic Changes in the Gene Expression Patterns and Lipid Profiles in the Developing and Maturing Meibomian Glands. Int J Mol Sci 23, 7884. https://doi.org/10.3390/ijms23147884.

Butovich, I.A., Wilkerson, A., Yuksel, S., 2023. Dysregulation of Lipid Metabolism in Aging Meibomian Glands and Its Molecular Markers. Int J Mol Sci 24. https://doi.org/10.3390/ijms241713512.

Cursiefen, C., Schlotzer-Schrehardt, U., Holbach, L.M., Pfeiffer, R.A., Naumann, G.O., 1999. Ocular findings in ichthyosis follicularis, atrichia, and photophobia syndrome. Arch Ophthalmol 117, 681-684. https://doi.org/10.1001/archopht.117.5.681.

Hamm, H., Meinecke, P., Traupe, H., 1991. Further delineation of the ichthyosis follicularis, atrichia, and photophobia syndrome. Eur J Pediatr 150, 627-629. https://doi.org/10.1007/BF02072621.

Lin, C.W., Lin, M.Y., Huang, J.W., Wang, T.J., Lin, I.C., 2024. Impact of dry eye disease treatment on patient quality of life. Front Med (Lausanne) 11, 1305579. https://doi.org/10.3389/fmed.2024.1305579.

Mizuno, Y., Yamada, M., Shigeyasu, C., 2012. Annual direct cost of dry eye in Japan. Clin Ophthalmol 6, 755-760. https://doi.org/10.2147/OPTH.S30625.

Narang, P., Donthineni, P.R., D'Souza, S., Basu, S., 2023. Evaporative dry eye disease due to meibomian gland dysfunction: Preferred practice pattern guidelines for diagnosis and treatment. Indian J Ophthalmol 71, 1348-1356. https://doi.org/10.4103/IJO.IJO_2841_22.

Patel, S., Nelson, D.R., Gibbs, A.G., 2001. Chemical and physical analyses of wax ester properties. J Insect Sci 1, 4. https://doi.org/10.1673/031.001.0401.

Stapleton, F., Argueso, P., Asbell, P., Azar, D., Bosworth, C., Chen, W., Ciolino, J., Craig, J.P., Gallar, J., Galor, A., Gomes, J.A.P., Jalbert, I., Jie, Y., Jones, L., Konomi, K., Liu, Y., Merayo-Lloves, J., Oliveira, F.R., Quinones, V.A.P., Rocha, E.M., Sullivan, B.D., Sullivan, D.A., Vehof, J., Vitale, S., Willcox, M., Wolffsohn, J., Dogru, M., 2025. TFOS DEWS III Digest Report. Am J Ophthalmol. https://doi.org/10.1016/j.ajo.2025.05.040.

Valdes-Arias, D., Locatelli, E.V.T., Sepulveda-Beltran, P.A., Mangwani-Mordani, S., Navia, J.C., Galor, A., 2024. Recent United States Developments in the Pharmacological Treatment of Dry Eye Disease. Drugs 84, 549-563. https://doi.org/10.1007/s40265-024-02031-6.

Wang, H., Humbatova, A., Liu, Y., Qin, W., Lee, M., Cesarato, N., Kortum, F., Kumar, S., Romano, M.T., Dai, S., Mo, R., Sivalingam, S., Motameny, S., Wu, Y., Wang, X., Niu, X., Geng, S., Bornholdt, D., Kroisel, P.M., Tadini, G., Walter, S.D., Hauck, F., Girisha, K.M., Calza, A.M., Bottani, A., Altmuller, J., Buness, A., Yang, S., Sun, X., Ma, L., Kutsche, K., Grzeschik, K.H., Betz, R.C., Lin, Z., 2020. Mutations in SREBF1, Encoding Sterol Regulatory Element Binding Transcription Factor 1, Cause Autosomal-Dominant IFAP Syndrome. Am J Hum Genet 107, 34-45. https://doi.org/10.1016/j.ajhg.2020.05.006.

Yu, J., Asche, C.V., Fairchild, C.J., 2011. The economic burden of dry eye disease in the United States: a decision tree analysis. Cornea 30, 379-387. https://doi.org/10.1097/ICO.0b013e3181f7f363.

Figure 1

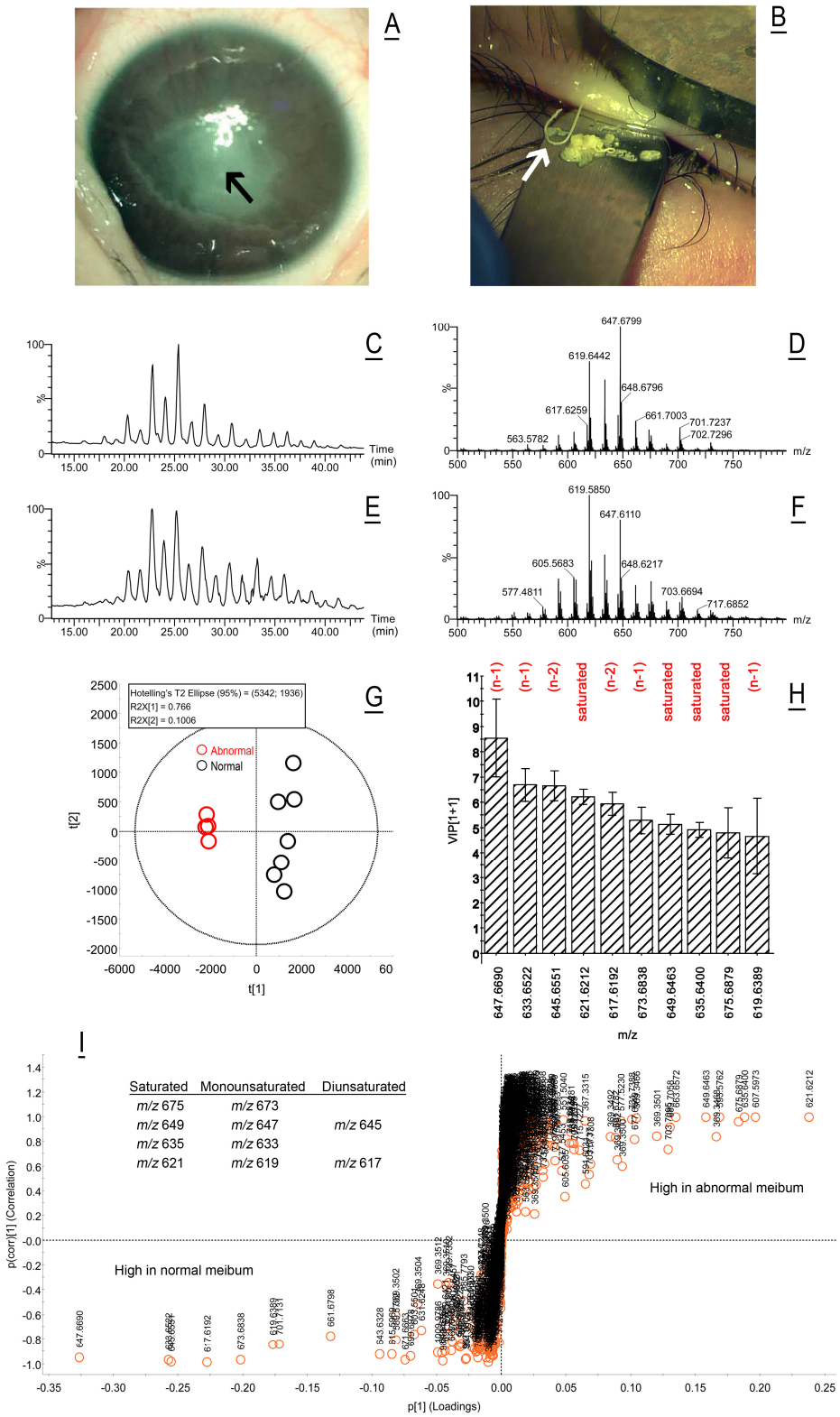
A
B
C
D
E
F
G
H
I
Time (min)
m/z
647.6799
619.6442
648.6796
617.6259
661.7003
701.7237
702.7296
563.5782
619.5850
647.6110
605.5683
648.6217
577.4811
703.6694
717.6852
Hotelling's T2 Ellipse (95%) = (5342; 1936)
R2X[1] = 0.766
R2X[2] = 0.1006
Abnormal
Normal
t[1]
t[2]
VIP[1+1]
(n-1)
(n-2)
saturated
647.6690
633.6522
645.6551
621.6212
617.6192
673.6838
649.6463
635.6400
675.6879
619.6389
Saturated Monounsaturated Diunsaturated
m/z 675 m/z 673
m/z 649 m/z 647 m/z 645
m/z 635 m/z 633
m/z 621 m/z 619 m/z 617
High in abnormal meibum
High in normal meibum
p(corr)[1] (Correlation)
p[1] (Loadings)

Figure 2

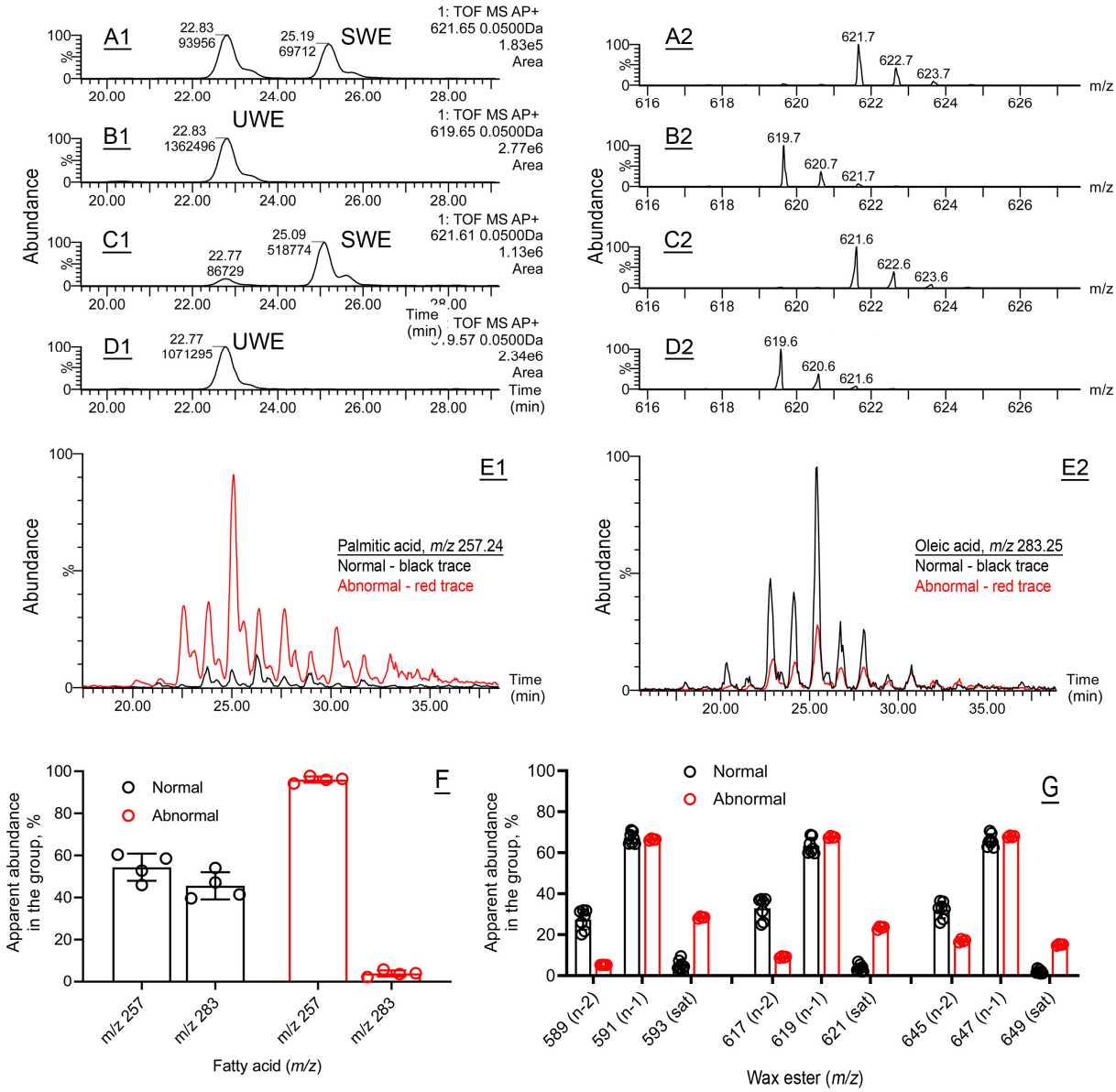
A1
22.83
93956
25.19
69712
SWE
1: TOF MS AP+
621.65 0.0500Da
1.83e5
Area
B1
22.83
1362496
UWE
1: TOF MS AP+
619.65 0.0500Da
2.77e6
Area
C1
22.77
86729
25.09
518774
SWE
1: TOF MS AP+
621.61 0.0500Da
1.13e6
Area
D1
22.77
1071295
UWE
2.34e6
Area
Abundance
Time (min)
A2
621.7
622.7
623.7
B2
619.7
620.7
621.7
C2
621.6
622.6
623.6
D2
619.6
620.6
621.6
m/z
E1
Palmitic acid, m/z 257.24
Normal - black trace
Abnormal - red trace
E2
Oleic acid, m/z 283.25
Normal - black trace
Abnormal - red trace
F
Normal
Abnormal
Apparent abundance in the group, %
m/z 257
m/z 283
m/z 257
m/z 283
Fatty acid (m/z)
G
589 (n-2)
591 (n-1)
593 (sat)
617 (n-2)
619 (n-1)
621 (sat)
645 (n-2)
647 (n-1)
649 (sat)
Wax ester (m/z)